

05,08

Investigation of the propagation of spin waves in the corrugated waveguide—planar waveguide system when changing the modulation parameters

© V.A. Gubanov, A.V. Kostrikin, A.V. Sadovnikov

Saratov National Research State University,
Saratov, Russia

E-mail: vladmeen@gmail.com

Received April 17, 2023

Revised April 17, 2023

Accepted May 11, 2023

The influence of the period filling parameter in the lateral system planar waveguide/corrugated waveguide is investigated by the method of micromagnetic modeling. The modes of switching the propagation of spin waves to the output ports are shown. When a defective region is added to the system — a region without periodicity — the transmission spectrum changes, and additional frequency regions of wave transmission appear. Based on the results obtained, it is possible to create a directional coupler applicable to information signal processing devices based on the principles of magnonics.

Keywords: spin waves, magnonica, defect, ferromagnet, depth of grooves.

DOI: 10.61011/PSS.2023.07.56401.43H

1. Introduction

Currently, creation of a base of complementary interconnecting devices on magnonic principles [1] is of great interest in order to implement new data signal processing devices. Spin waves (SW) serve as data carriers [2]. High variability of connection of elementary magnetic units allow to create a set of functional units [3].

Yttrium-iron garnet (YIG) ferromagnetic film featuring a record-low damping parameter are the best medium for SW propagation [4]. YIG films may be obtained by the liquid-phase epitaxy methods [5] or laser deposition technique [6]. Minimum film thicknesses suitable for SW propagation may reach dozens of nanometers.

Spin wave can be controlled by varying system parameters such as external magnetic field direction and strength, frequency and power of SW signal excited in the system and by introduction of additional control parameters in the system — application of deformations [7], laser emission induction [8], imposing metallized surfaces on the ferromagnetic waveguide.

Also, creation of an irregular profile of the waveguiding structure is one of the SW parameter control options. For example — creation of periodic irregularities forming magnon crystals (periodic conditions for profile variation along the waveguiding structure thickness) or corrugated waveguides (periodic profile variation conditions over the waveguide width) [9]. Depending on geometrical parameters of spin wave signal period and excitation frequency, conditions will occur when the incident and reflected waves in the periodicity domain will be opposite in phase, and will result in damping of spin wave propagation.

The study will investigate, using the micromagnetic simulation method, the SW propagation modes in the coupled waveguide structure system, one of which is a planar waveguide and the other is a corrugated waveguide without and with a defective region. SW power redistribution conditions between the output ports of the coupled structure will be investigated. This structure may be used as a directional coupler of spin wave signal to create microwave signal processing devices on magnonic principles.

2. Studied structures and numerical simulation procedure

The studied structure is a system of laterally coupled waveguides — planar waveguide and corrugated waveguide with similar width (shown in Figure 1, *a*) with parameters for the YIG film: saturation magnetization $M_0 = 139$ G. A region without periodicity was created in the corrugated waveguide, hereinafter referred as the defect, which will be shown in Figure 1, *b* and highlighted in orange color. The defective segment length was equal to $l_{\text{def}} = 1000 \mu\text{m}$.

These coupled waveguides have the following parameters: structure length $l = 6000 \mu\text{m}$, structure width $w = 500 \mu\text{m}$, groove depth a was varied from 40 to 60 μm , waveguide thickness was equal to $t = 10 \mu\text{m}$. The waveguide structures were placed along the long axis of the waveguide and with spacing of $d = 15 \mu\text{m}$.

For this structure, overlapping parameter was optimized $L = h + k$, where k is the corrugation „ridge“ length, and h is the groove length. In further discussion, the overlapping parameter was equal to $L = 160 \mu\text{m}$ ($h = 80 \mu\text{m}$, $k = 80 \mu\text{m}$).

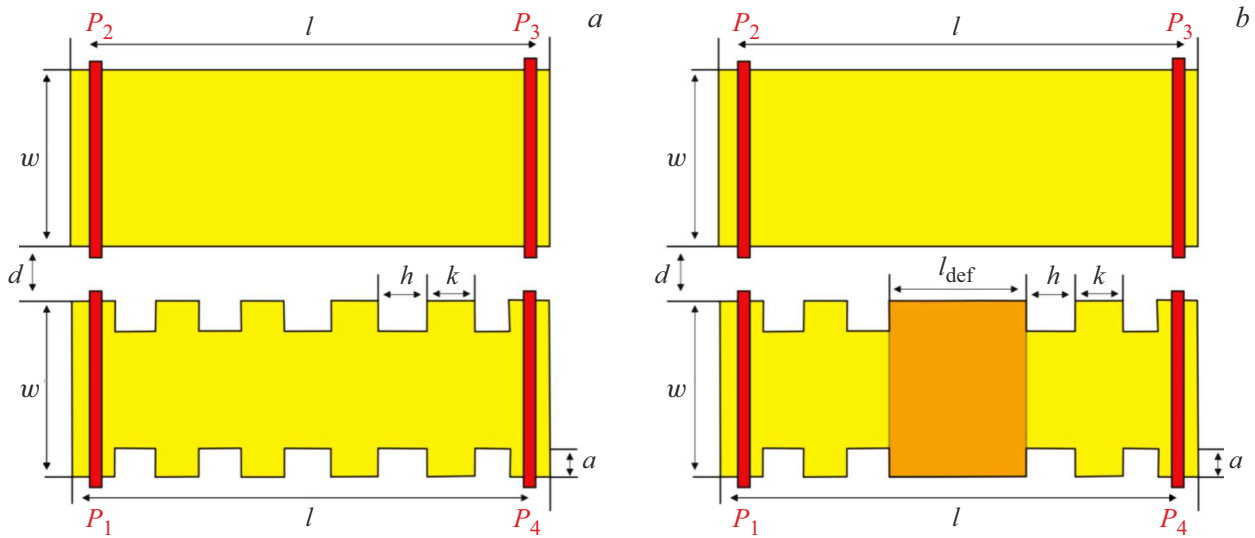


Figure 1. Image of the studied lateral structure planar waveguide/corrugated waveguide without addition of a defective region (a) and with addition of a defective region into the corrugated waveguide region (b).

Micromagnetic simulation created conditions for excitation of magnetostatic surface wave (MSSW) when external magnetic field H_0 with strength 1200 Oe was applied along the y axis.

This system of waveguide structures has 4 ports which were placed over the width of each of the waveguides. Port P_1 served as an input microstrip on which the spin wave was excited. Ports P_2 , P_3 and P_4 served as receivers of propagating spin waves. Widths of these antennas were equal to $30\ \mu\text{m}$.

The study was carried out in MuMax³ software package [10], where the simulated structure had a $1024 \times 256 \times 1$ ($L \times W \times D$) grid in whose points the Landau–Lifshitz equation with the Hilbert damping was solved numerically [11,12]:

$$\frac{\partial \mathbf{M}}{\partial t} = \gamma [\mathbf{H}_{\text{eff}} \times \mathbf{M}] + \frac{\alpha}{M_s(x,y)} \left[\mathbf{M} \times \frac{\partial \mathbf{M}}{\partial t} \right], \quad (1)$$

where \mathbf{M} is the magnetization vector, $\alpha=10^{-5}$ is the YIG film damping parameter, $\mathbf{H}_{\text{eff}} = \mathbf{H}_0 + \mathbf{H}_{\text{demag}} + \mathbf{H}_{\text{ex}} + \mathbf{H}_a$ is the effective magnetic field, \mathbf{H}_0 is the external magnetic field, $\mathbf{H}_{\text{demag}}$ is the demagnetization field, \mathbf{H}_{ex} is the exchange field, \mathbf{H}_a is the anisotropy field, $\gamma = 2.8\ \text{MHz/Oe}$ is the gyromagnetic ratio. Spin wave was excited as follows: $h_z(t) = h_0 \text{sinc}(2\pi ft)$, where f is the spin wave excitation frequency, $h_0 = 0.1\ \text{Oe}$. Then the dynamic magnetization $m_z(x, y, t)$ in the output antenna regions P_2 , P_3 , P_4 was recorded with step $\Delta t = 75\ \text{fs}$ during $t = 200\ \text{ns}$. And further, one-dimensional Fourier transformations were performed using the obtained data and as a result amplitude-frequency characteristics (AFC) were obtained for the propagating spin waves.

Figure 2 shows AFC for parameter $a = 40\ \mu\text{m}$ (Figure 2, a) and parameter $a = 60\ \mu\text{m}$ (Figure 2, c) without

introduction of defective region l_{def} and for parameter $a = 40\ \mu\text{m}$ (Figure 2, b) and parameter $a = 60\ \mu\text{m}$ (Figure 2, d) with introduction of defective region l_{def} . To obtain AFC, a signal was applied to the input port P_1 (brown line) and removed from input ports P_2 (green line), P_3 (blue line) and P_4 (red line) in the simulated structure.

These AFC suggest that the transfer characteristics are transformed and frequency range displacement with dips is observed. In this case, only when the depth of the corrugated waveguide is changed a from 40 to $60\ \mu\text{m}$ in the frequency range 5.22 – $5.3\ \text{GHz}$, spin wave power distribution occurs into the output port P_3 into the output port P_4 .

When a defective region is introduced, AFC of the corrugated waveguide structure (Figure 2, b, d), when the corrugated waveguide depth is changed a from 40 to $60\ \mu\text{m}$, frequency tuning region broadening from $\Delta f = 80$ to $170\ \text{MHz}$ (range 5.21 – $5.38\ \text{GHz}$) was observed.

For the dips observed on AFC using micromagnetic simulation, spatial maps of distribution of m_z component and spin wave intensity $I = \sqrt{m_z^2 + m_x^2}$ were plotted for different parameters a without defective region addition (Figure 3) and with defective region addition (Figure 4).

At $f = 5.28\ \text{GHz}$ (Figure 3, a, b) with $a = 40\ \mu\text{m}$, a mode is observed when the spin wave is transferred into the planar waveguide and back to the corrugated waveguide. In this case, conditions occur in the planar waveguide for propagation of the second spin wave width mode.

When a increases up to $60\ \mu\text{m}$ at $f = 5.25\ \text{GHz}$ (Figure 3, c, d), spin wave power transfer and output via the output port P_3 are implemented.

When a defective region is added to the corrugated waveguide during plotting of the maps of distribution of m_z component and spin wave intensity at the dip-specific frequency, conditions can be implemented when

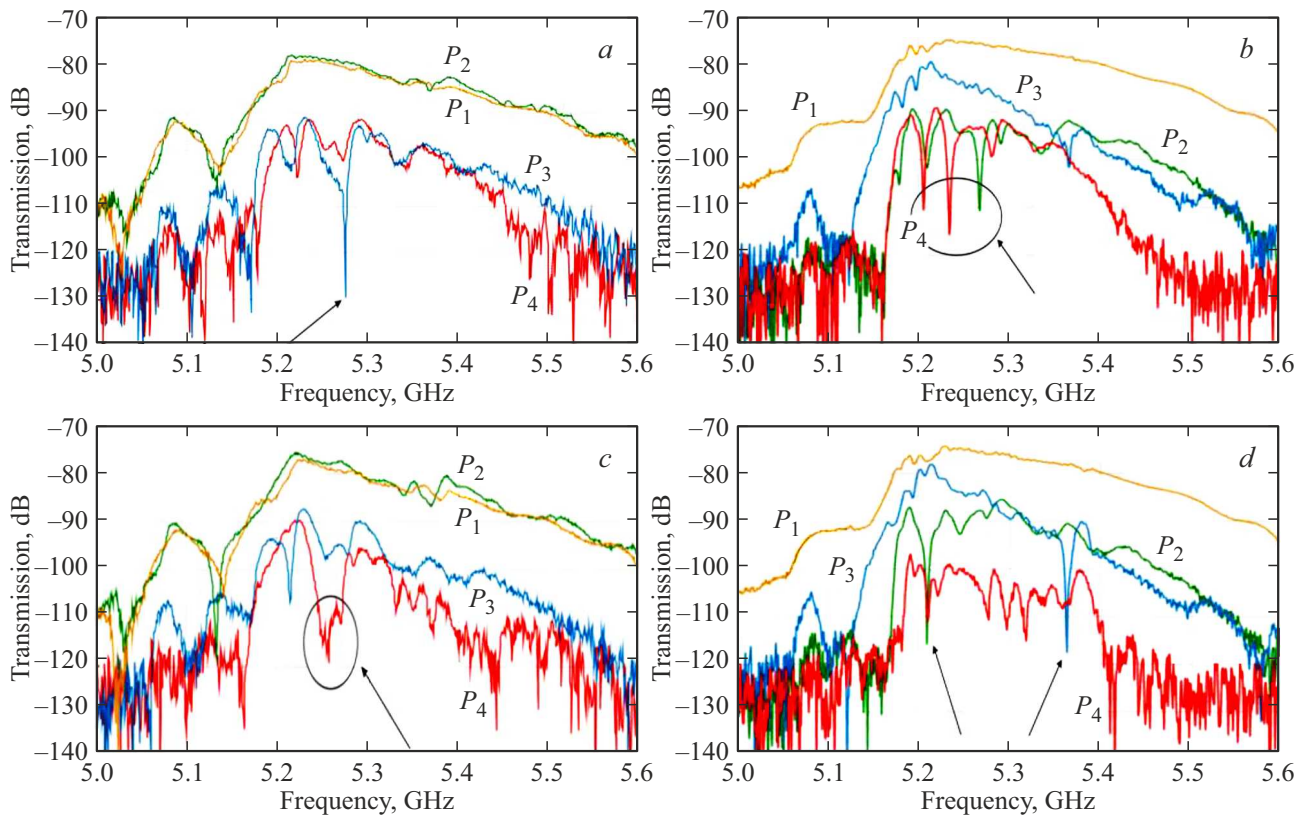


Figure 2. Amplitude-frequency characteristics for parameter $a = 40\ \mu\text{m}$ (Figure 2.a) and parameter $a = 60\ \mu\text{m}$ (Figure 2.c) without introduction of defective region l_{def} and for parameter $a = 40\ \mu\text{m}$ (Figure 2.b) and parameter $a = 60\ \mu\text{m}$ (Figure 2.d) with introduction of defective region l_{def} . To obtain the amplitude-frequency characteristics, a signal was applied to the input port P_1 (brown line) and removed from input ports P_2 (green line), P_3 (blue line) and P_4 (red line) in the simulated structure.

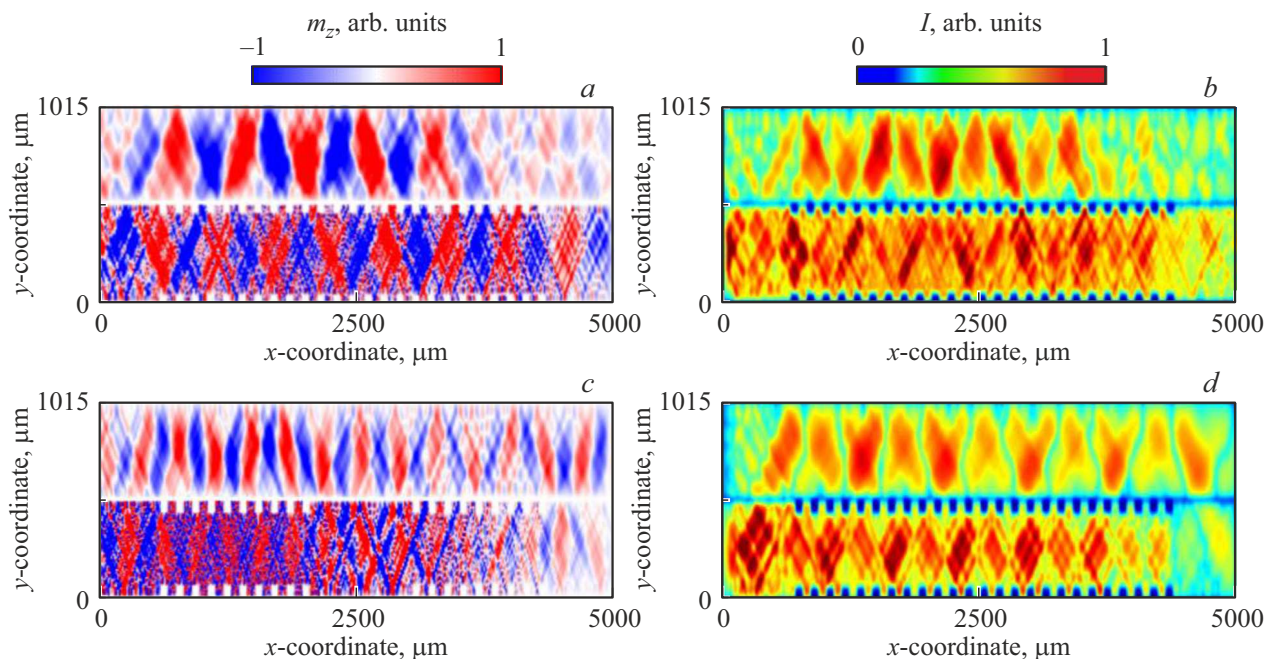


Figure 3. Spatial distribution maps m_z SW magnetization and intensity components in the system without defective region at $f = 5.28\ \text{GHz}$ (a, b) with $a = 40\ \mu\text{m}$ and with $a = 60\ \mu\text{m}$ at $f = 5.25\ \text{GHz}$ (c, d).

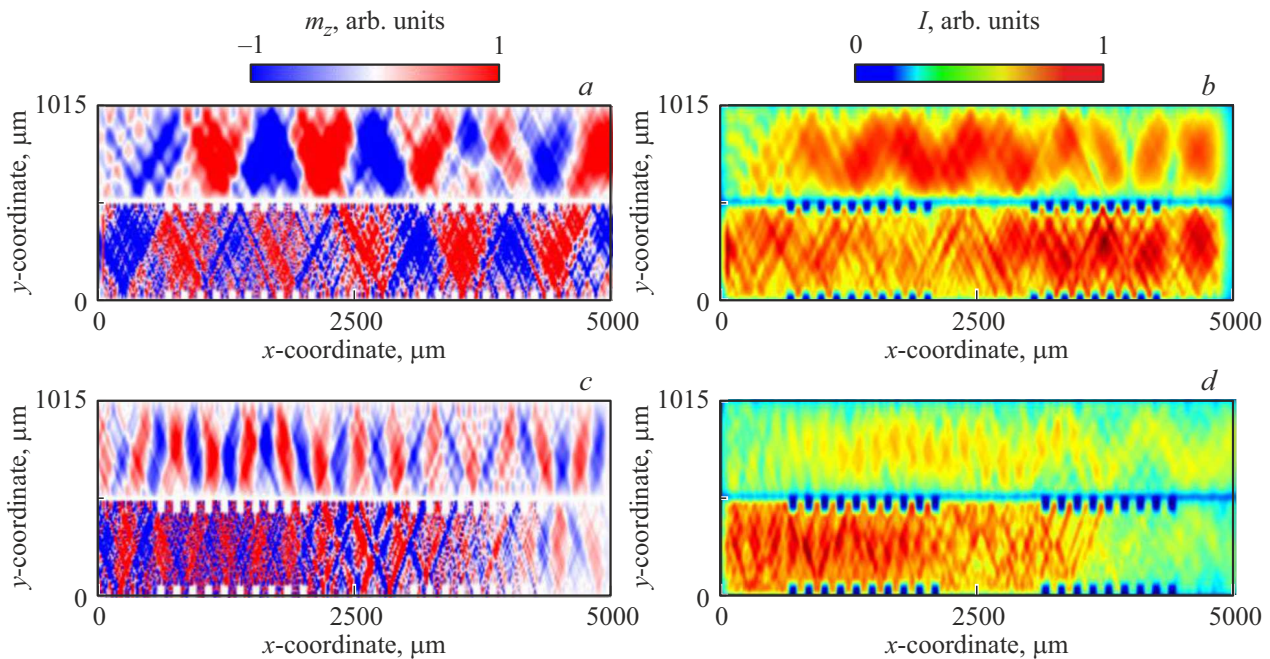


Figure 4. Spatial distribution maps m_z SW magnetization and intensity components in the system with defective region at $f = 5.23$ GHz (*a, b*) with $a = 40 \mu\text{m}$ and with $a = 60 \mu\text{m}$ at $f = 5.36$ GHz (*c, d*).

the spin wave is redistributed between the output ports P_3 and P_4 (Figure 4, *a, b*) at 5.23 GHz, or spots redistributing (Figure 4, *c, d*) at 5.36 GHz providing conditions for SW reflection from the defect boundary.

3. Conclusion

Thus, a coupled structure planar waveguide–corrugated waveguide was investigated using numerical simulation. transfer characteristics and spatial maps of distribution of m_z magnetization component and spin wave intensity were plotted to demonstrate the SW power redistribution conditions. When a defective region without periodicity was added into the corrugated waveguide, additional frequencies occur in the system to redirect the SW power. This structure may be used as a directional microwave signal coupler to create data signal processing devices on magnonic principles.

Funding

The study was performed with the support of the Ministry of Education and Science of Russia as part of the Government Task (project No. FSRR-2023-0008).

Conflict of interest

The authors declare that they have no conflict of interest.

References

- [1] S.A. Nikitov, D.V. Kalyabin, I.V. Lisenkov, A.N. Slavin, Y.N. Barabanenkov, S.A. Osokin, A.V. Sadovnikov, E.N. Beginin, M.A. Morozova, Y.P. Sharaevsky, Y.A. Filimonov, Y.V. Khivintsev, S.L. Vysotsky, V.K. Sakharov, E.S. Pavlov. *Phys.-Usp.* **58**, 1002 (2015).
- [2] V. Demidov, S. Urazhdin, G. de Loubens, O. Klein, V. Cros, A. Anane, S. Demokritov. *Phys. Rep.* **673**, 1 (2017).
- [3] C.S. Davies, A.V. Sadovnikov, S.V. Grishin, Y.P. Sharaevsky, S.A. Nikitov, V.V. Kruglyak. *IEEE Transact. Magn.* **51**, 1 (2015).
- [4] V. Cherepanov, I. Kolokolov, V. Lvov. *Phys. Rep.* **229**, 81 (1993).
- [5] C. Dubs, O. Surzhenko, R. Thomas, J. Osten, T. Schneider, K. Lenz, J. Grenzer, R. Hübner, E. Wendler. *Phys. Rev. Mater.* **4**, 024416 (2020).
- [6] L.V. Lutsev, A.M. Korovin, S.M. Sutorin, L.S. Vlasenko, M.P. Volkov, N.S. Sokolov. *J. Phys. D* **53**, 265003 (2020).
- [7] V. Sadovnikov, A.A. Grachev, S.E. Sheshukova, Y.P. Sharaevskii, A.A. Serdobintsev, D.M. Mitin, S. A. Nikitov. *Phys. Rev. Lett.* **120**, 257203 (2018).
- [8] M. Vogel, A.V. Chumak, E.H. Waller, T. Langner, V.I. Vasyuchka, B. Hillebrands, G. von Freymann. *Nature Phys.* **11**, 487 (2015).
- [9] S. Nikitov, P. Tailhades, C. Tsai. *J. Magn. Magn. Mater.* **236**, 320 (2001).
- [10] A. Vansteenkiste, J. Leliaert, M. Dvornik, M. Helsen, F. Garcia-Sanchez, B.V. Waeyenberge. *AIP Adv.* **4**, 107133 (2014).
- [11] L. Landau, E. Lifshitz. *Phys. Z Sowj* **8**, 153 (1935).
- [12] T.L. Gilbert, J.M. Kelly. *American Institute of Electrical Engineers* **253–263** (1955).

Translated by Ego Translating